Proceedings of the Combustion Institute 40 (2024) 105205

Contents lists available at ScienceDirect

Proceedings of the Combustion Institute

journal homepage: www.elsevier.com/locate/proci

Flame stabilization by a highly conductive cylinder: Multiple steady-state solutions and dynamics

Anne Dejoan, Carmen Jiménez, Vadim N. Kurdyumov *

Energy Department, CIEMAT, Madrid, Spain

ARTICLE INFO

Keywords:
Premixed flame stabilization
Bluff-body
Flame dynamics
Multiplicity of steady-state solutions
Heat recirculation

ABSTRACT

This study examines stabilization of a premixed flame by a circular cylinder placed perpendicularly to the uniform flow of the reacting mixture. It is assumed that the cylinder has a high thermal conductivity leading to an effectively uniform surface temperature. This temperature is not fixed, but it is determined by a thermal flame-cylinder balance. The numerical investigation is carried out on the basis of low Mach number Navier–Stokes equations coupled with the conservation equations for the energy and the fuel mass. Two models for transport coefficients are compared. The first model assumes they have constant values, and the second takes into account their change with temperature.

Numerical modeling shows that within the specific range of parameters of this study the system can have several steady-state solutions corresponding to different cylinder temperatures. Moreover, at least two solutions are shown to be stable, corresponding to the hottest and coldest cylinder temperatures. The actual occurrence of one or another regime depends on the initial conditions.

1. Introduction

Combustion in a closed system is accompanied by the interaction of the flame with the surrounding solid parts, such as a porous plug used for injecting a flammable mixture or the walls of the device. An important issue is the interaction with a bluff body placed in the reactants flow to achieve flame stabilization. Despite the fact that the systematic studies of this problem can be traced back more than 60 years [1–5] important aspects remain unexplored to this day.

The impact of a bluff body on the combustion field in the sense of flame stabilization occurs mainly for two reasons. The first one is the slowing down of the gas velocity in the vicinity of the solid. The second reason is the enhancement of heat transfer from products to reactants by heat transfer through the solid bluff body. The predominant configurations for numerical simulations found in literature are those of solid bodies placed in channels. Most of these investigations were carried out in the framework of two-dimensional models. The effect of solid materials on the blow-off limit of a micro-combustor was investigated in [6]. The influence of the flame holder temperature on the stabilization of a laminar methane flame by a cylinder was presented in [7]. Considerable effort has gone into modeling complex chemical kinetics [8–14] and conjugate heat transfer [12–17]. Flame stabilization behind the trailing edge of a semi-infinite cylindrical rod placed coaxially in a circular channel was investigated in [18].

The flame stabilization by means of a solid square maintained at a constant temperature in a laminar channel flow was studied in [19]. The problem of flame stabilizing in a uniform flow by means of a circular cylinder was considered in [20]. In particular, it was found that when the temperature of the cylinder is not fixed and is determined by interaction with the flame, then up to five non-trivial steady-state solutions can be observed at certain parameter values. These multiple steady-state solutions correspond to a zero value of the net heat flux between the gas and the surface of the bluff body.

The results presented in [20] were based on a thermo-diffusive combustion model. The main weakness of this approximation is the assumption of constant density. In the present study, this physical problem is investigated taking into account the effect of thermal expansion, which modifies the gas velocity field around the cylinder. The study is based on the Navier–Stokes equations coupled with the equations of conservation of energy and fuel mass.

2. Formulation and numerical treatment

A circular cylinder of radius R is placed perpendicularly to an incoming flow of a combustible mixture at initial temperature T_0, density ρ_0 and fuel mass fraction Y_0 moving with a uniform velocity U_0 far upstream relative to the cylinder. It is assumed that the flame speed

* Corresponding author.
E-mail address: vadim.k@ciemat.es (V.N. Kurdyumov).

https://doi.org/10.1016/j.proci.2024.105205
Received 30 November 2023; Accepted 29 May 2024
Available online 24 June 2024

of the corresponding planar flame, S_L, is smaller than the velocity of the mixture, $S_L < U_0$. This condition prevents upstream flame propagation. Within this configuration, the flame can be stabilized only under the action of the cylinder, which works like a flame holder. In the present study, the problem statement is limited to a two-dimensional consideration and all solutions are assumed to be mirror-symmetric about the x-axis. Thus, all dependent variables are functions of the spatial variables r and ϕ, where $x' = r'\cos\phi$, $y' = r'\sin\phi$ and $0 < \phi < \pi$. Here the "x'"-axis coincides with the direction of initial gas flow and the "y'"-axis is perpendicular to this direction. Primes here and hereafter mark dimensional quantities if the same notation is used for dimensional and non-dimensional variables. The subindex "0" indicates initial fresh stream values.

The combustion process is modeled by a global, one step and irreversible reaction of the form $F + O \rightarrow P + Q$, where F, O and P denote the fuel, the oxidizer and the products, respectively, and Q is the heat released per unit mass of fuel. We assume for simplicity that the mixture is lean in fuel and consider the oxidizer mass fraction as constant. Then, the reaction proceeds at the rate $\Omega = \mathcal{B}\rho'^2 Y' \exp(-\mathcal{E}/\mathcal{R}T)$, where $\mathcal{B}$ is pre-exponential factor containing the oxidizer mass fraction, ρ' is the mixture density, Y' is the fuel mass fraction, $\mathcal{E}$ is the overall activation energy, $\mathcal{R}$ is the universal gas constant and T is the temperature. The same kinetics were used in [20] within the constant density model. However, it should be noted here that the reaction rate is proportional to the product of the concentrations of fuel and oxidizer. This is why the reaction rate is proportional to ρ'^2 despite the fact that the oxidizer consumption is neglected.

In this work, two well-known models for the reactant gas mixture transport coefficients are used. In the first model, all coefficients are assumed to be constant. In the second, more general model, the temperature dependence of the viscosity, η, the thermal conductivity, λ, and the fuel diffusivity, D, are approximated by a power law of the form $\eta/\eta_0 = \lambda/\lambda_0 = \rho D/\rho_0 D_0 = (T/T_0)^\sigma$. In the present work the heat capacity, c_p, is assumed to be constant. A typical value for σ is usually chosen as $\sigma = 0.7$. This model for the transport properties is similar to that proposed in [21], where the Prandtl number $Pr = \eta c_p/\lambda$ and the Lewis number $Le = \lambda/(\rho c_p D)$ were assumed to have constant values. Note that the first model is a special case of the second one with $\sigma = 0$.

Dimensionless variables are defined as follows

$$\begin{aligned} &t = t'U_0/R,\ x = x'/R,\ y = y'/R,\\ &\mathbf{v} = \mathbf{v}'/U_0,\ \rho = \rho'/\rho_0,\ Y = Y'/Y_0,\\ &\theta = (T - T_0)/(T_a - T_0),\ p = p'/(\rho_0 U_0^2), \end{aligned} \tag{1}$$

where $\mathbf{v}' = v'_\phi \mathbf{e}_\phi + v'_r \mathbf{e}_r$ is the velocity vector, p' is the manometric pressure and $T_a = T_0 + QY_0/c_p$ is the adiabatic flame temperature.

The combustion field is determined by the coupled continuity, momentum, energy and fuel balance equations. The gas governing equations and the equation of state take the form

$$\rho_t + \nabla(\rho\mathbf{v}) = 0, \tag{2}$$

$$\rho\mathbf{v}_t + \rho(\mathbf{v}\nabla)\mathbf{v} = -\nabla p + \nabla\tau/Re, \tag{3}$$

$$\rho\theta_t + \rho(\mathbf{v}\nabla)\theta = [\nabla(\mu\nabla\theta) + \omega]/RePr, \tag{4}$$

$$\rho Y_t + \rho(\mathbf{v}\nabla)Y = [\nabla(\mu\nabla Y)/Le - \omega]/RePr, \tag{5}$$

$$\rho(1 + q\theta) = 1, \tag{6}$$

where $\mu = (1 + q\theta)^\sigma$, with $q = (T_a - T_0)/T_0$ the heat release parameter, $\tau = \mu[\nabla\mathbf{v} + \nabla^T\mathbf{v} - 2\mathbf{I}(\nabla\mathbf{v})/3]$ is the dimensionless viscous stress tensor, and $Re = \rho_0 U_0 R/\eta_0$ is the Reynolds number. Since typical Mach numbers in most applications are small compared with unity, we have neglected the pressure variations in the equation of state. We have also neglected the viscous dissipation in the energy equation.

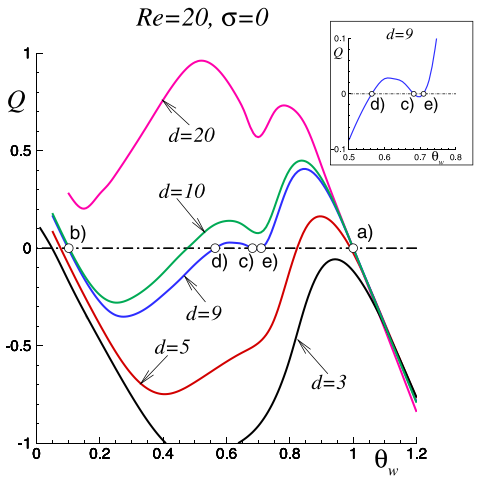

Fig. 1. The calculated Q values determining the heat flux in Eq. (8) plotted as a function of θ_w for $Re = 20$, $\sigma = 0$ and various d. The inset shows the interval of θ_w in which additional roots of the equation $Q = 0$ appear for $d = 9$.

The non-dimensional reaction rate, $\omega = \Omega R/\rho_0 U_0$, is given by

$$\omega = \frac{d\beta^2(1+q)^{2-\sigma}\rho^2 Y}{2Le\,u_p^2}\exp\left\{\frac{\beta(\theta-1)}{(1+q\theta)/(1+q)}\right\}, \tag{7}$$

where $\beta = \mathcal{E}(T_a - T_0)/\mathcal{R}T_a^2$ and $d = R^2/\delta_T^2$ are the Zel'dovich and Damköhler numbers, respectively. The Damköhler number is the square of the ratio of the cylinder radius to the thermal width of a planar flame, $\delta_T = \lambda_0/(c_p\rho_0 S_L)$. This expression for the reaction rate is obtained when the usual Arrhenius reaction rate is written in dimensionless form.

The factor $u_p = S_L/S_L^{as}$ included in Eq. (7) ensures that the non-dimensional speed of a planar adiabatic flame equals unity for a given finite β, where S_L^{as} is the asymptotic value of adiabatic laminar flame speed calculated at $\beta \rightarrow \infty$:

$$S_L^{as} = \sqrt{2(\lambda_0/c_p)Le\beta^{-2}\mathcal{B}\rho_0^{n-2}(T_a/T_0)^{\sigma-n}} \times \exp(-E/2\mathcal{R}T_a)$$

According to Bush and Fendell [22], $u_p = 1 + a_1/\beta + \ldots$, as $\beta \rightarrow \infty$. The numerical values of u_p calculated by a shooting method are given in [23].

In this work we assume that the thermal conductivity of the solid material is much higher than that of the gas. The temperature of the cylinder remains uniform in this limit, being a function of time only. A formal mathematical discussion of this approximation is given in [20]. Denoting the temperature of the cylinder as θ_w, to be determined, and the local heat flux on the cylinder surface as $q_L(\phi) = \mu(\theta_w)\partial\theta/\partial r|_{r=1}$, the energy balance equation for the cylinder becomes

$$C\frac{d\theta_w}{dt} = Q, \tag{8}$$

where $Q = \int_0^\pi q_L(\phi)d\phi$, the total heat flux to the cylinder, is a function of θ_w. Here $C = \pi R c_w \rho_w U_0/(2\lambda_0)$ represents the total dimensionless thermal capacity of the cylinder. This value is based on the density and heat capacity of the cylinder material (averaged over the cross section of the cylinder) ρ_w and c_w, respectively. In realistic cases of metal flame holders, for example, this parameter should be much greater than one. However, it is obvious that its value can be easily changed experimentally by layer-by-layer combination of materials with different ρ_w and c_w, for example.

The boundary conditions for the temperature and mass fraction on the cylinder surface become:

$$r = 1:\ \theta = \theta_w,\ \partial Y/\partial r = 0,\ \mathbf{v} = 0. \tag{9}$$

On the x-axis, standard symmetry conditions are assumed:

$$\phi = 0, \pi \; : \; \frac{\partial \theta}{\partial r} = \frac{\partial Y}{\partial r} = \frac{\partial v_r}{\partial \phi} = v_\phi = 0 \, . \tag{10}$$

In a similar way as in [20], the solution of the above problem was carried out in two stages. Firstly, the problem of finding a stabilized flame at a given and fixed cylinder temperature θ_w was solved numerically. The solution to this problem determines the total heat flux to the cylinder appearing in Eq. (8) as a function of the cylinder temperature, $Q = F(\theta_w)$. It should be noted that the results obtained for a cylinder with a fixed temperature are interesting in themselves from the point of view of flame stabilization by heated bodies. Although in most cases time-dependent solutions were brought to stationary states, oscillatory modes were also observed for some parameter values.

It is obvious that the values of the temperature for which the total heat flux to the cylinder is equal to zero determine the steady states corresponding to the flame holder (cylinder) thermally insulated from the external environment interacting only with the flame. Alternatively, at the second stage, the coupled time-dependent system of equations Eqs. (2)–(6) and (8) was solved numerically. One can expect that the time dynamics depends on the parameter C, but the steady state solutions (if they exist) are independent of this parameter.

For the calculations presented below, the set of dimensionless time-dependent Eqs. (2)–(6) was resolved making use of the open source code OpenFoam [24]. The implemented numerical method was based on the finite volume method formulated in a collocated grid arrangement. A first order Euler scheme was used for temporal discretization and a second-order centered scheme for spatial discretization. The computational domain is discretized into a block-structured mesh: a radial distribution is used within a radius $3R$ around the cylinder with a homogeneous grid resolution, $h_r = 0.075$; far away from the cylinder, a Cartesian mesh is used with a maximum grid resolution value of 0.1 in both the longitudinal and vertical directions. The domain size extends from -6 to 50 along the x-direction and from 0 to 50 along the y-direction. The grid resolution ensures 5 to 10 points in the thermal flame thickness δ_T, depending on the value of the Damkhöler number considered. We checked the independence of the solution from the grid resolution and mesh decomposition by increasing the grid resolution by a factor 2 and also by further extending the radial mesh distribution around the cylinder up to $6R$.

All the results presented below were obtained for $Le = 1$. The Prandtl number was assigned a constant value $Pr = 0.72$. The values of the Zel'dovich number and heat release parameter were chosen as $\beta = 10$ and $q = 5$, which are typical values used to represent the combustion of lean methane-air mixtures, for example.

3. Results

3.1. Solutions for the cylinder with a fixed temperature

Let us first consider the steady-state solutions obtained for the model with constant transport coefficients, $\sigma = 0$. Fig. 1 shows the dependence of the total heat flux Q into the cylinder appearing in Eq. (8) on its temperature, θ_w, calculated for $Re = 20$ and various values of the Damköhler number d. The main interest is to determine the cylinder temperature values that give $Q = 0$, corresponding to the steady states for a cylinder in contact only with the flame, that is, without heat loss to the environment.

Fig. 1 demonstrates that for sufficiently high values of the Damköhler number (*e.g* the curve plotted for $d = 20$), there is only one steady state for which $Q = 0$. This state corresponds to a temperature of the cylinder close to the adiabatic flame temperature, $\theta_w \approx 1$. In contrast, for sufficiently low values of d (*e.g.* the $d = 3$ curve), only one steady state is possible with $Q = 0$ but it corresponds to a nearly cold cylinder, $\theta_w \lesssim 0.1$.

One can see in Fig. 1 that at intermediate values of the Damköhler number, two states corresponding to $Q = 0$ exist simultaneously,

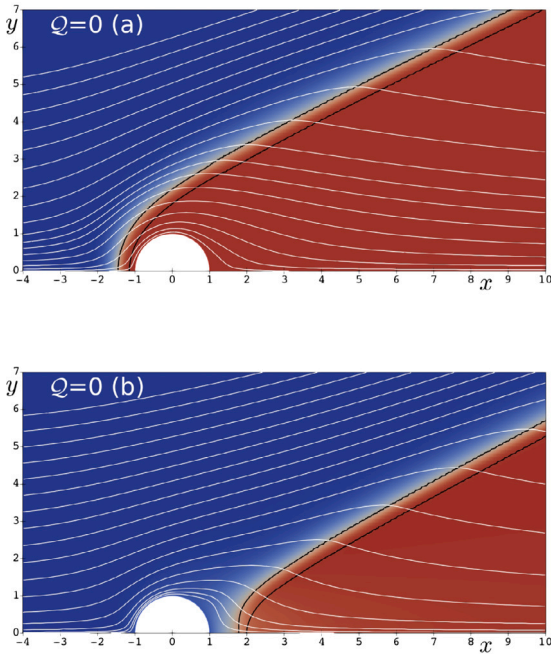

Fig. 2. Example of the solutions with the highest and lowest values of θ_w for points (a) and (b) corresponding to $Q = 0$ in Fig. 1 for the case $d = 9$. The color shades represent the temperature field, white lines show the streamlines and the isoline $\omega = 0.35$ is marked with a black line. (For interpretation of the references to color in this figure legend, the reader is referred to the web version of this article.)

with cold and hot cylinder temperatures. As a consequence of this, in view of the obvious physical fact that the curve Q versus θ_w must be continuous, a third steady state must appear, corresponding to an intermediate cylinder temperature. Moreover, for some values of d, two additional states with $Q = 0$ appear, which are illustrated by the curve with $d = 9$. It should be noted, however, that the emergence of two additional solutions takes place in a narrow range of the Damköhler number. The hot and cold cylinder modes are denoted below as (a) and (b), respectively, while the intermediate states are denoted by (c), (d) and (e), as marked in Fig. 1 for the case with $d = 9$.

It is interesting to note that the results obtained on the basis of the full Navier Stokes equations (with variable density) Eqs. (2)–(6) are in good qualitative agreement with the results presented in [20] where the constant density approximation was applied. This qualitative agreement is obtained even for the effect of the appearance of two additional states, as for the case with $d = 9$ in Fig. 1. This indicates that the effect of the thermal interaction between the flame and the cylinder plays a leading role in the process of flame stabilization. Some quantitative differences between the constant density model and the model used in the present study may lie in the definition of the Damköhler number, since the reaction rate given by Eq. (7) depends on the square of the density.

Fig. 2 illustrates the steady-state solutions ($Q = 0$) obtained for the hottest and coldest values of the cylinder temperature marked by points (a) and (b) in Fig. 1 for the case with $d = 9$. Note that the numerical domain for calculations significantly exceeds that shown in the figures. It can be seen that for the solution with the hottest cylinder temperature, $\theta_w \approx 1$, namely solution (a), the flame envelops the cylinder. For solution (b), the flame is located behind the cylinder, leaving it relatively cold, $\theta_w \approx 0.1$.

Fig. 3 shows three steady state solutions corresponding to intermediate values of the cylinder temperature. Since the values of θ_w are close to each other, the distributions of the variables are very similar to each other. It can be seen that the flame impacts on the cylinder at an angle ϕ approximately equal to $\pi/2$. It is worth noting that this case, namely the

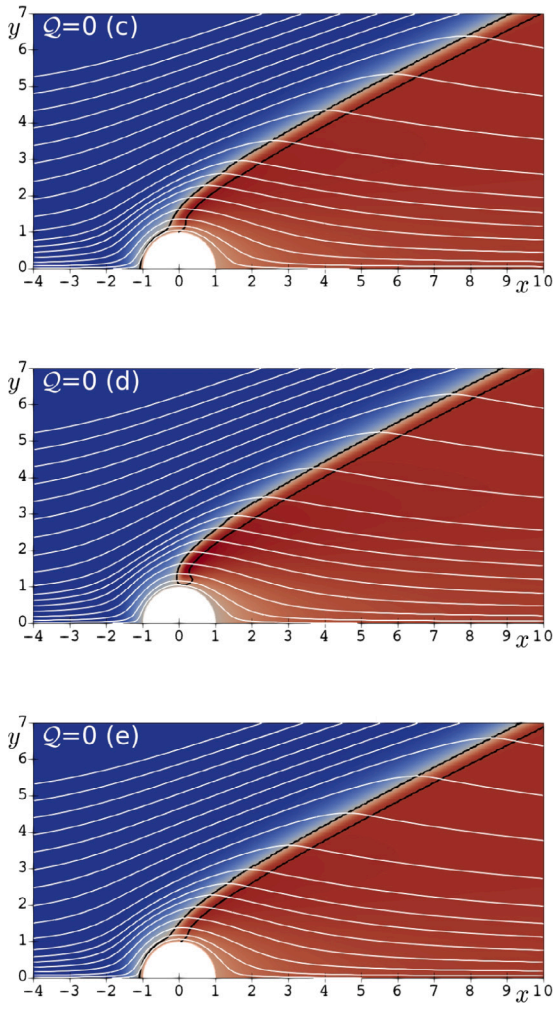

Fig. 3. Example of the solutions with intermediate temperatures corresponding to points (c), (d) and (e) in Fig. 1 for the case $d = 9$ corresponding to $\mathcal{Q} = 0$. The color shades illustrate the temperature field, white lines show the streamlines and the isoline $\omega = 0.35$ is marked with a black line. (For interpretation of the references to color in this figure legend, the reader is referred to the web version of this article.)

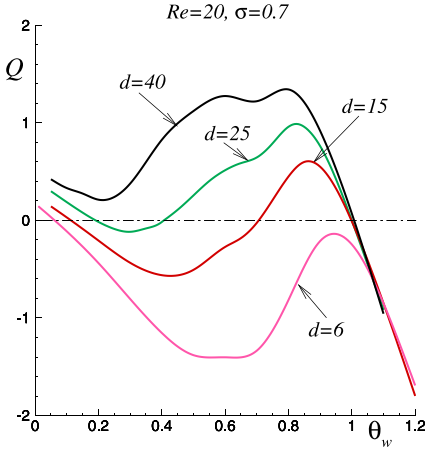

Fig. 4. The calculated $\mathcal{Q}$ values appearing in Eq. (8) plotted as a function of θ_w for $Re = 20$, $\sigma = 0.7$ and various d.

existence of three intermediate steady-state solutions corresponding to $\mathcal{Q} = 0$, is a special one because it is observed only within a narrow range of the Damköhler number. A less special situation is the case of only one

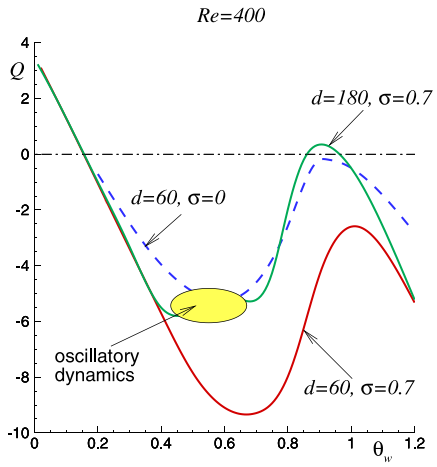

Fig. 5. The calculated $\mathcal{Q}$ values appearing in Eq. (8) plotted as a function of θ_w for $Re = 400$. The approximate region of oscillatory dynamics is marked with an oval in the figure.

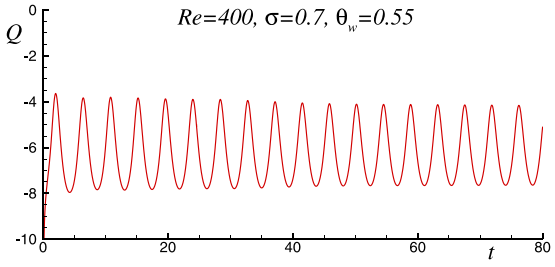

Fig. 6. An example of oscillatory behavior obtained at a fixed cylinder temperature, for $\theta_w = 0.55$, $Re = 400$, $d = 180$ and $\sigma = 0.7$.

intermediate mode corresponding to $\mathcal{Q} = 0$, represented by curves with $d = 5$ and $d = 10$ in Fig. 1. Anticipating the results of time-dependent calculations with non-fixed cylinder temperature, one can notice that these steady-state modes are unstable. Namely, states (d) and (e) are always absolutely unstable, while for state (c) the temperature of the cylinder experiences relatively small oscillations around the steady-state value. It should also be added that this time-dependent dynamics depends on the value of the parameter C appearing in Eq. (8).

Fig. 4 shows the response curves obtained within the model with $\sigma = 0.7$ calculated for $Re = 20$. It can be seen that the qualitative behavior of the curves remains similar to the case with $\sigma = 0$. For the small value $d = 6$, there is only one solution, with slight heating of the cylinder. For sufficiently large d, the curve plotted with $d = 40$, the only solution is a regime with a cylinder temperature close to adiabatic. And there is also an interval of Damköhler numbers when these solutions can exist simultaneously. In this case, an intermediate regime appears, which, anticipating the results of time-dependent calculations, is unstable. The only difference between the solutions with $\sigma = 0$ and $\sigma = 0.7$ is that in the second case the two additional solutions with $\mathcal{Q} = 0$ do not appear.

The results presented above were obtained for a fairly low Reynolds number, $Re = 20$. Numerical calculations have shown that the existence of at least three different regimes in a certain range of Damköhler numbers persists also at much higher Reynolds numbers. Fig. 5 shows the response curves obtained for $Re = 400$. The solid curves were obtained with Damköhler numbers equal to $d = 60$ and $d = 180$ for the model with $\sigma = 0.7$. For comparison, the dashed curve shows the response curve obtained for $d = 60$ and $\sigma = 0$. It can be seen that the tendency obtained at lower Reynolds numbers (multiplicity of steady-state solutions corresponding to $\mathcal{Q} = 0$) also persists for higher Re.

For all the above calculations with fixed cylinder temperatures carried out for $Re = 20$, a time-independent solution was established

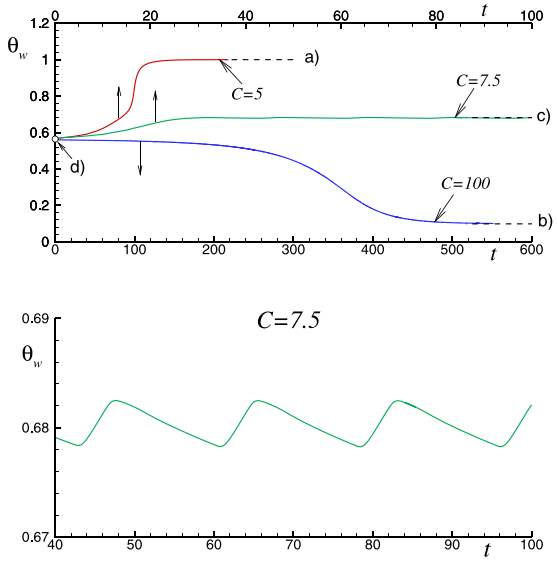

Fig. 7. The upper plot shows time histories of the cylinder temperature obtained after small perturbations of the state (d) chosen as the initial conditions. Dashed lines show the cylinder temperature for steady states. The lower plot illustrates low amplitude oscillatory dynamics.

after a transition period. However, for $Re = 400$, oscillatory behavior was observed within a small range of θ_w. An example of such behavior is illustrated in Fig. 6, where the total heat flux into the cylinder is plotted as a function of time for $Re = 400$, $d = 180$, $\sigma = 0.7$ and $\theta_w = 0.55$. It should be noted that the obtained oscillatory modes were found in the range of the cylinder temperature where the total heat flux $\mathcal{Q}$ is noticeably different from zero.

3.2. Solution for the cylinder with non-fixed temperature

All the above results were obtained for cases with a fixed cylinder temperature. In a mathematical sense, this corresponds to the limit $C \to \infty$ in Eq. (8). At finite values of the parameter C, Eq. (8) should be taken into account and the cylinder temperature varies with time.

Carrying out time-dependent calculations under arbitrary initial conditions would have a limited interest. Instead, small perturbations were introduced into the distributions of variables obtained at a fixed cylinder temperature and corresponding to $\mathcal{Q} = 0$. The resulting distributions were chosen as initial conditions for calculations with a finite value of C in Eq. (8). The main purpose of these calculations was to find out whether a given steady-state solution corresponding to the condition $\mathcal{Q} = 0$ is stable or not.

There is a well known method to draw a conclusion about the stability of a particular steady state (corresponding to the condition $\mathcal{Q} = 0$) based on the profile of the response curve. Indeed, if the function $\mathcal{Q} = \mathcal{F}(\theta_w)$ is given, and $\mathcal{F}(\theta_{w0}) = 0$ is fulfilled, then, based on Eq. (8), one could conclude that if $d\mathcal{F}/d\theta_w|_{\theta_w=\theta_{w0}} < 0$, then the state with $\theta_w = \theta_{w0}$ is stable. Typical reasoning usually says that if the cylinder temperature increases slightly (randomly), the heat flux to the cylinder decreases and its temperature should then decrease to its original state corresponding to the $\mathcal{Q} = 0$ state. Conversely, with a small perturbation resulting in a decrease of the cylinder temperature, the heat flux increases and the cylinder heats up, returning again to the initial temperature θ_{w0}.

However, as it was demonstrated in [20] within the constant density model, this method may not lead to a correct conclusion about the stability of the steady states corresponding to $\mathcal{Q} = 0$. Firstly, a situation is possible when, at a given (fixed) $\theta_w = \theta_{w0}$, oscillatory flame dynamics takes place. Let us assume that the shape of the response curve corresponds to a negative slope at this point. However, since an oscillatory mode occurs at $\theta_w = \theta_{w0}$, if the amplitude of the oscillations is sufficiently large, the system switches to one of the stable states, cold or hot, depending on the initial disturbances introduced.

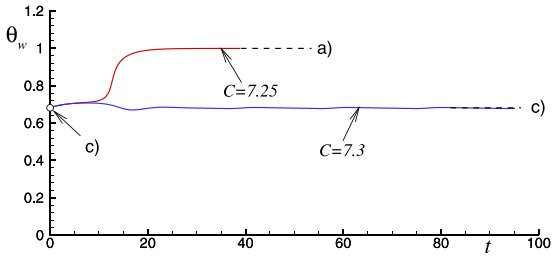

Fig. 8. Time history after small perturbations of state (c). At sufficiently small values of C, the system approaches the hot mode (a), but at C greater than a certain critical value, the system experiences oscillatory dynamics.

Secondly, the stability of the state with $\theta_w = \theta_{w0}$ may depend on the value of the parameter C. A similar situation was reported in [25], where the stabilization of a flame in a channel in the presence of a highly conductive wall segment and its interaction with the flame were studied. It is this case that was observed also in the present study. Fig. 7 shows the time history of the cylinder temperature for one of the cases with $d = 9$ (see Fig. 1), the intermediate case (d). A small disturbance was applied to θ_w and Eqs. (2)–(6) were calculated together with Eq. (8) using as initial conditions the solution (d) and different values of C.

One can see in the upper plot of Fig. 7, calculated for $Re = 20$ and $\sigma = 0$, that for $C = 5$, the system approaches the hot state (a) after a transition period, while for $C = 100$, the cylinder temperature approaches the cold state (b). It is interesting to note that for the intermediate value, $C = 7.5$, the cylinder temperature experiences small oscillatory dynamics around state (c). This oscillatory behavior is illustrated in the lower plot of Fig. 7. Of course, these results cannot give an exhaustive answer to the question of which is the stable state to which the system transitions to when it is perturbed, since this also depends on the magnitude of the initial perturbation. However, one can conclude confidently that states (a) and (b), namely the hottest and coldest states of the cylinder, are both stable. At the same time, these calculations show that state (d) is unstable. The same conclusion about the instability of state (e) can be made (the time history of this case is not included here for brevity).

The time histories related to perturbations of state (c) are illustrated in Fig. 8 for two values of the parameter C. It can be seen that the steady state (c) is oscillatory unstable for sufficiently large values of the parameter C, but the amplitude of cylinder temperature oscillations are similar to those shown in Fig. 7. However, for values of the parameter C below a critical value, a transition to the hot state (a) occurs. Thus, we can conclude that the intuitive method for determining stability based on the slope of the response curve gives the correct answer only for the steady-state solutions corresponding to the hottest and coldest cylinder temperatures.

4. Conclusions and discussions

In this work, we conducted the study of flame stabilization by a bluff body, a cylinder, located perpendicularly in a homogeneous flow of the combustible mixture within the framework of a model described by the Navier–Stokes equations with variable density combined with the equations of conservation of energy and mass of the fuel. It is also assumed that the thermal conductivity of the cylinder is so high that its temperature is uniform. The main attention is focused on the cases where the cylinder is in contact only with the flame and is isolated from the external environment. Therefore, the cylinder temperature is determined as part of the solution to the problem.

Numerical calculations have shown that at a sufficiently high intensity of the combustion process, (high Damköhler number), the flame-cylinder system ends up in a state where the cylinder temperature is close to the adiabatic temperature of the flame. At a low combustion intensity (small Damköhler number), the flame is located behind the cylinder and its temperature is relatively low, about one tenth of the adiabatic flame temperature.

The most interesting result of this work is the confirmation of the existence of a fairly wide intermediate range of Damköhler numbers when hot and cold regimes exist simultaneously. Moreover, time-dependent numerical calculations showed that the hottest and coldest solutions turn out to be both stable, that is, each of them can be achieved under appropriate initial conditions. It is also interesting that the results obtained are in good agreement with previous research based on a constant density model [20]. It is also shown that the results obtained are robust with respect to the model for the transport coefficients. This indicates that the main cause of the solution multiplicity effect is the thermal interaction of the flame with the cylinder. In this case, the flow modification due to thermal expansion may play a secondary role. It can also be assumed that the multiplicity effect will most likely persist at Reynolds numbers greater than $Re = 400$ studied in the present work, including at turbulent regimes. However, this should be tested on appropriate models.

Although the time-dependent calculations presented in this work are important for answering the question of the stability of steady states, the main research method is the calculation of the combustion field for a given and fixed cylinder temperature θ_w. Knowing the temperature field already, the heat flux into the cylinder is easily determined, providing the response curve $Q = \mathcal{F}(\theta_w)$. The resulting response curve allows us to determine all the steady-state states, including unstable states, as the states corresponding to zero heat flux, that is, the roots of the equation $\mathcal{F}(\theta_w) = 0$.

The proposed procedure for finding solutions makes it easy to generalize the problem and also to take into account possible heat losses from the cylinder to the environment. To do this, one just need to include in Eq. (8) an additional term, $Cd\theta_w/dt = \mathcal{F}(\theta_w) - S$, where S is the corresponding heat sink term, while $\mathcal{F}(\theta_w)$ remains the same.

Novelty and significance statement

The novelty of this work lies in the fact that for the first time the possibility of multiplicity of flames stabilized using a bluff body (a cylinder) based on the Navier-Stokes equations associated with the equations of balance of energy and fuel mass is demonstrated. The investigation was carried out within the approximation of high thermal conductivity of the cylinder, which implies a uniform surface temperature unknown beforehand. Dynamic states are governed by time-dependent calculations of the gas mixture equations coupled with the heat balance equation of the cylinder. The steady state solutions are determined by zero total heat flux to the cylinder. Using numerical modeling, the existence of hot and cold modes for the same set of parameters is demonstrated. The results are significant when applied to flame stabilization in combustion devices.

CRediT authorship contribution statement

Anne Dejoan: Designed research, Performed research, Analyzed data, Writing – original draft. **Carmen Jiménez:** Designed research, Performed research, Analyzed data, Writing – original draft. **Vadim N. Kurdyumov:** Designed research, Performed research, Analyzed data, Writing – original draft.

Declaration of competing interest

The authors declare that they have no known competing financial interests or personal relationships that could have appeared to influence the work reported in this paper.

Acknowledgments

This study was supported by project GREEN-H2 from CAM and MICIU with funding from European Union NextGenerationEU (PRTR-C17.I1) as well by #PID2022-139082NB-C52 MCIN/ AEI /10.13039/ 501100011033/ and FEDER.

References

[1] S.I. Cheng, A.A. Kovitz, Theory of flame stabilization by a bluff body, Proc. Combust. Inst. 7 (1958) 681–891.
[2] F.H. Wright, Some aerodynamics factors influencing bluff body flame stabilization, Combust. Flame 2 (1958) 96–97.
[3] F.H. Wright, Bluff-body flame stabilization - blockage effects, Combust. Flame 3 (1959) 319–337.
[4] T. Maxworthy, On the mechanism of bluff body flame stabilization at low velocities, Combust. Flame 6 (1962) 233–244.
[5] K.M. Kundu, D. Banerjee, D. Bhaduri, Theoretical analysis on flame stabilization by a bluff-body, Combust. Sci. Tech. 17 (1977) 153–162.
[6] A. Fan, J. Wan, K. Maruta, H. Yao, W. Liu, Interactions between heat transfer, flow field and flame stabilization in a micro-combustor with a bluff body, Int. J. Heat Mass Trans. 66 (2013) 72–79.
[7] M. Miguel-Brebion, D. Mejia, P. Xavier, F. Duchaine, B. Bedat, L. Selle, T. Poinsot, Joint experimental and numerical study of the influence of flame holder temperature on the stabilization of a laminar methane flame on a cylinder, Combust. Flame 172 (2016) 153–161.
[8] K. Kedia, C. Safta, J. Ray, H. Najm, A. Ghoniem, A second-order coupled immersed boundary-SAMR construction for chemically reacting flow over a heat-conducting Cartesian grid-conforming solid, J. Comput. Phys. 272 (2014) 408–428.
[9] K. Kedia, A. Ghoniem, The anchoring mechanism of a bluff-body stabilized laminar premixed flame, Combust. Flame 161 (2014) 327–339.
[10] K.S. Kedia, A.F. Ghoniem, The blow-off mechanism of bluff-body stabilized laminar premixed flame, Combust. Flame 162 (2015) 1304–1315.
[11] K.S. Kedia, A.F. Ghoniem, The response of a hamonically forced premixed flame stabilized on a heatconducting bluff-body, Combust. Flame 35 (2015) 1065–1072.
[12] C. Jiménez, D. Michaels, A. Ghoniem, Stabilization of ultra-lean hydrogen enriched inverted flames behind a bluff-body and the phenomenon of anomalous blow-off, Combust. Flame 191 (2018) 86–98.
[13] C. Jiménez, D. Michaels, A. Ghoniem, Ultra-lean hydrogen-enriched oscillating flames behind a heat conducting bluff-body: Anomalous and normal blow–off, Proc. Combust. Ins. 37 (2019) 1843–1850.
[14] Y. Yan, Z. He, Q. Xu, L. Zhang, L. Li, Zh Yang, J. Ran, Numerical study on premixed hydrogen/air combustion characteristics in microcombustor with slits on both sides of the bluff body, Int. J. Hydr. Eng. 44 (1919) 1998–2012.
[15] P. Xavier, A. Ghani, D. Mejia, M. Miguel-Brebion, M. Bauerheim, L. Selle, T. Poinsot, Experimental and numerical investigation of flames stabilised behind rotating cylinders: Interaction of fames with a moving wall, J. Fluid Mech. 813 (2017) 127–151.
[16] D. Mejia, M. Bauerheim, P. Xavier, B. Ferret, L. Selle, T. Poinsot, Stabilization of a premixed laminar flame on a rotating cylinder, Proc. Combust. Inst. 36 (2017) 1447–1455.
[17] D. Mejia, M. Miguel-Brebion, A. Ghani, T. Kaiser, F. Duchaine, L. Selle, T. Poinsot, Influence of flame-holder temperature on the acoustic flame transfer functions of a laminar flame, Combust. Flame 188 (2018) 5–12.
[18] V.N. Kurdyumov, Y.L. Shoshin, L.P.H. de Goey, Structure and stability of premixed flames stabilized behind the trailing edge of a cylindrical rod at low Lewis numbers, Proc. Combust. Ins. 35 (2015) 981–988.
[19] S. Berger, F. Duchaine, L.Y.M. Gicquel, Bluff-body thermal property and initial state effects on a laminar premixed flame anchoring pattern, Flow Turb. Combust. 100 (2018) 561–591.
[20] V.N. Kurdyumov, C. Jiménez, Flame stabilisation by a highly conductive body: Multiple steady-state solutions and time dependent dynamics, Combust. Theor. Modell. 26 (2022) 669–685.
[21] M.D. Smooke, V. Giovangigli, in: M.D. Smooke (Ed.), Reduced Kinetic Mechanisms and Asymptotic Approximations for Methane-Air Flames, Springer-Verlag, Berlin, 1990, pp. 1–28.
[22] W.B. Bush, F.E. Fendell, Asymptotic analysis of laminar flame propagation for general Lewis number, Combust. Sci. Technol. 1 (1970) 421–428.
[23] V.N. Kurdyumov, Propagation of premixed isobaric flames in narrow channels with heat-losses: The asymptotic analysis revised and reliance on the flame-sheet model, Combust. Flame 206 (2019) 138–149.
[24] http://www.openfoam.com.
[25] V.N. Kurdyumov, C. Jiménez, Flame stabilization in narrow channels by a highly conductive wall segment: Application to small-scale combustion devices, Combust. Flame 245 (2022) 112348.